

## Aberystwyth University

### *Knickpoint evolution in a supraglacial stream*

Kamintzis, Jayne Elizabeth; Irvine-Fynn, Tristram; Holt, Thomas; Jones, John Paul Pryderi; Tooth, Stephen; Griffiths, Hywel; Hubbard, Bryn

*Published in:*

Geografiska Annaler: Series A, Physical Geography

*DOI:*

[10.1080/04353676.2018.1549945](https://doi.org/10.1080/04353676.2018.1549945)

*Publication date:*

2019

*Citation for published version (APA):*

Kamintzis, J. E., Irvine-Fynn, T., Holt, T., Jones, J. P. P., Tooth, S., Griffiths, H., & Hubbard, B. (2019). Knickpoint evolution in a supraglacial stream. *Geografiska Annaler: Series A, Physical Geography*, 101(2), 118-135. <https://doi.org/10.1080/04353676.2018.1549945>

#### **General rights**

Copyright and moral rights for the publications made accessible in the Aberystwyth Research Portal (the Institutional Repository) are retained by the authors and/or other copyright owners and it is a condition of accessing publications that users recognise and abide by the legal requirements associated with these rights.

- Users may download and print one copy of any publication from the Aberystwyth Research Portal for the purpose of private study or research.
- You may not further distribute the material or use it for any profit-making activity or commercial gain
- You may freely distribute the URL identifying the publication in the Aberystwyth Research Portal

#### **Take down policy**

If you believe that this document breaches copyright please contact us providing details, and we will remove access to the work immediately and investigate your claim.

tel: +44 1970 62 2400  
email: [is@aber.ac.uk](mailto:is@aber.ac.uk)

## 1 **Knickpoint evolution in a supraglacial stream**

2 Kamintzis, J.E. <sup>1\*</sup>, Irvine-Fynn, T.D.L.<sup>1</sup>, Holt, T.O. <sup>1</sup>, Jones, J.P.P. <sup>2</sup>, Tooth, S.<sup>1</sup>,  
3 Griffiths, H.<sup>1</sup> and Hubbard, B.<sup>1</sup>

4 <sup>1</sup>*Department of Geography and Earth Sciences, Aberystwyth University, Aberystwyth, SY23*  
5 *3DB, Wales, UK.*

6 <sup>2</sup>*Deri Jones & Associates, Ltd., Llwyngwyn, Forge, Machynlleth, SY20 8RR, Wales, UK.*

7  
8 \* Email: jek12@aber.ac.uk

9  
10 Tristram David Linton Irvine-Fynn – [tdi@aber.ac.uk](mailto:tdi@aber.ac.uk), 01970622784, ORCID: [http://orcid.org/0000-](http://orcid.org/0000-0003-3157-6646)  
11 [0003-3157-6646](http://orcid.org/0003-3157-6646)

12 Thomas Owen Holt – [toh08@aber.ac.uk](mailto:toh08@aber.ac.uk), 01970628449, ORCID: [https://orcid.org/0000-0001-8361-](https://orcid.org/0000-0001-8361-0688)  
13 [0688](https://orcid.org/0000-0001-8361-0688), @tom\_holt

14 John Paul Pryderi Jones – [deri@djaweb.co.uk](mailto:deri@djaweb.co.uk), 01654702001, @deri\_jones

15 Stephen Tooth – [set@aber.ac.uk](mailto:set@aber.ac.uk), 01970622361, ORCID: <https://orcid.org/0000-0001-5714-2606>

16 Hywel Griffiths – [hmg@aber.ac.uk](mailto:hmg@aber.ac.uk), 09170622674, ORCID: <https://orcid.org/0000-0002-0480-2014>,  
17 @HywelGriffiths

18 Bryn Hubbard – [byh@aber.ac.uk](mailto:byh@aber.ac.uk), 01970622783, ORCID: <https://orcid.org/0000-0002-3565-3875>,  
19 @Bryn\_Hubbard

20  
21 Word count – 9426

22

23

24

25

## Knickpoint evolution in a supraglacial stream

Despite numerous studies of knickpoints in bedrock and alluvial channels, no detailed description of knickpoint change on ice has been reported to date. This paper presents the first investigation of knickpoint evolution within a supraglacial stream. Repeat longitudinal profile surveys of a knickpoint on Vadrec del Forno, Switzerland reveal a step height increase of 115 mm and upstream migration of 0.26 m over three days during the 2017 ablation season. Rates and magnitudes of erosion vary spatially across the knickpoint in relation to differing discharge regimes. At high discharges ( $\sim 0.013 \text{ m}^3 \text{ s}^{-1}$ ), erosion is focused at the step base; at low discharges ( $\sim 0.003 \text{ m}^3 \text{ s}^{-1}$ ), erosion is focused on the reach upstream of the knickpoint, at the step lip and the step-riser face. This results in replacement of knickpoint morphology, driven by frictional thermal erosion and hydraulic action. Pool formation further influences step morphology, inducing secondary circulation and increased melt at the base of the step-riser, causing steepening. Results highlight the complexities of water flow over knickpoints, demonstrating that the stream power law does not accurately characterise changing knickpoint morphology or predict retreat rates. Although morphological similarities have been reported between supraglacial and bedrock/alluvial channels, knickpoints in non-ice-walled channels will not necessarily respond to discharge similarly to those in ice due to the different erosion processes involved.

Keywords: knickpoint; step; supraglacial; evolution; hydrodynamics; discharge

### 1. Introduction

Knickpoints are commonly observed features in the longitudinal profile of river channel systems. The term 'knickpoint' refers to channel reaches that exhibit a marked change in bed slope, and is used herein to refer to an individual step, comprising the local point of abrupt gradient change (the step lip) and the downstream channel-spanning steep segment (the 'step-riser'; Chartrand and Whiting 2000). Such changes in slope have been attributed to alterations in sediment supply (Brush and Wolman 1960) and base-level change resulting from eustatic, geological or tectonic perturbations (Haviv et al. 2010), with their presence increasing hydraulic resistance and dissipating energy (Leopold et al. 1960; Abrahams et al. 1995; Curran and Wohl 2003; Wilcox et al. 2011). Most knickpoints undergo upstream migration, governing

56 wider landscape changes through alteration of hillslope base level (Tucker and Whipple 2002;  
57 Bigi et al. 2006; Whittaker and Boulton 2012). Three types of knickpoint retreat have been  
58 identified by Gardner (1983) using flume experiments in cohesive, homogenous substrates: (i)  
59 *parallel retreat* with retention of the original step morphology; (ii) *replacement* with alteration  
60 of the original step morphology arising from erosion above the knickpoint lip and over the step  
61 face; and (iii) *backward rotation* of the step towards the general channel slope, causing the  
62 step-riser inclination to decrease. As adjustments in bedrock/alluvial channels typically occur  
63 over decadal-to-millennial timescales, direct observations of upstream knickpoint retreat are  
64 limited. Attempts have been made to predict knickpoint retreat rates in some landscapes using  
65 the stream power incision model (Bishop et al. 2005; Crosby and Whipple 2006; Berlin and  
66 Anderson 2007; Lague 2014). This model relates knickpoint retreat rate to catchment drainage  
67 size, which acts as a proxy for discharge (Whipple and Tucker 1999; Crosby and Whipple  
68 2006), assuming a constant flow regime. The stream power model, however, typically fails to  
69 predict observations of knickpoint retreat due to poor characterisation of changing flow  
70 regimes over a step (Dust and Wohl 2012), and the lack of consideration of sediment transport  
71 processes (Jansen et al. 2011), the role of bedrock structure (Mackey et al. 2014), plunge-pool  
72 dynamics (Scheingross and Lamb 2017) and the self-regulation of channel geometry (Baynes  
73 et al. 2018).

74         Within bedrock channels, there is a lack of empirical data describing actively migrating  
75 knickpoints (Cook et al. 2013), due to the typically slow retreat rates and difficulties in  
76 identifying and isolating controlling intrinsic and extrinsic factors (Kephart 2013). Knickpoint  
77 evolution mechanisms, therefore, remain poorly understood despite laboratory and flume  
78 studies investigating drivers of change (e.g. Bennet et al. 2000; Grimaud et al. 2015; Lamb et  
79 al. 2015; Baynes et al. 2018). However, knickpoint features have also been described in  
80 supraglacial (e.g. Knighton 1981, 1985; Carver et al. 1994; St Germain and Moorman 2016)

81 and englacial channels (e.g. Pulina 1984; Holmlund 1988; Griselin 1992; Vatne 2001; Piccini  
82 et al. 2002; Vatne and Refsnes 2003; Vatne and Irvine-Fynn 2016), where their formation is  
83 considered to be related to intrinsic flow dynamics, in contrast to extrinsic factors commonly  
84 cited for bedrock/alluvial systems (Phillips et al. 2010; Yokokawa et al. 2016). This gives rise  
85 to a unique field environment that allows for isolation of hydrodynamic variables, since  
86 ice-walled streams are typically devoid of sediment load (Leopold et al. 1960; Kostrzewski and  
87 Zwoliński 1995; Karlstrom et al. 2013), and channel boundaries are close to the melting point.  
88 These factors enable assessment of knickpoint evolution over shorter (hourly-to-diurnal)  
89 timescales. Supraglacial streams are often considered to be analogous to bedrock channels, due  
90 to their similarities in morphology and adjustment (Ewing 1970; Marston 1983; Knighton  
91 1985; Karlstrom et al. 2013) and, thus, supraglacial investigations have been used to gain a  
92 better empirical understanding of channel formation and evolution (Ferguson 1973).  
93 Constraining supraglacial knickpoint evolution also has implications for understanding  
94 englacial drainage systems, at least where conduits exist at atmospheric pressure, owing to  
95 knickpoints forming a major component of vertical channel incision (Gulley et al. 2009; Vatne  
96 and Irvine-Fynn 2016) and, thereby, underpinning meltwater transfer to a glacier's ice-bed  
97 interface.

98         Currently, the potential of the supraglacial environment for examining knickpoint  
99 formation and evolution processes has not yet been fulfilled. The majority of field-based  
100 research on supraglacial streams was published several decades ago (e.g. Ewing 1970;  
101 Pinchack 1972; Dozier 1974; Hambrey 1977), and focused on hydraulic geometry (e.g. Park  
102 1981; Marston 1983; Kostrzewski and Zwoliński 1995; Brykała 1999) or meandering (e.g.  
103 Knighton 1972; Ferguson 1973). Although the presence of knickpoints has been reported  
104 (Dozier 1974), the only study to address this morphology in any detail examined its role in  
105 inducing pulsating flow (St Germain and Moorman 2016). Despite a recent resurgence of

106 interest in supraglacial drainage, studies have predominantly used remotely sensed data (e.g.  
107 Joughin et al. 2013; Lampkin and VanderBerg 2014; Rippin et al. 2015; Smith et al. 2015;  
108 Karlstrom and Yang 2016; Yang et al. 2016) and, thus, do not account for a process-level  
109 understanding of local hydraulics. Therefore, there is a need to elucidate the processes  
110 responsible for morphological drainage evolution through field-based research (Gleason et al.  
111 2016), and to advance existing numerical models (e.g. Karlstrom et al. 2013; Mantelli et al.  
112 2015).

113 Here, we present repeat geometric measurements of a knickpoint within a supraglacial  
114 stream on Vadrec del Forno, Switzerland, to characterise its morphological evolution in  
115 response to hydrodynamic forcing. Measurement took place over three days during the 2017  
116 ablation season. The results provide the first description and quantification of changing  
117 knickpoint morphology on ice, and yield insight into the varying spatial focus of hydrological  
118 erosion at differing discharges.

## 119 **2. Field site**

120 Vadrec del Forno is a 4.5 km long, temperate, Alpine valley glacier located in the Bregaglia  
121 Range of Graubünden, southeast Switzerland (46°17'N, 9°40'E; Figure 1A). The glacier flows  
122 north from the Italian border, comprising two accumulation basins that form a shallow gradient,  
123 ~ 500 m wide tongue. The glacier elevation extended from ~ 2250 to 3200 m.a.s.l in 2016,  
124 covering an area of 5 km<sup>2</sup>. Across the ablation area, the predominant structural glaciological  
125 feature is longitudinal foliation (Jennings et al. 2014), exerting a strong control over surface  
126 meltwater drainage (cf. Hambrey 1977). This gives rise to relatively straight rills and streams  
127 flowing parallel to the glacier flow direction, providing an excellent site for examining  
128 hydrodynamics in straight channels unaffected by meander-induced secondary water  
129 circulation.

## 130        **2.1    *Channel reach and knickpoint characteristics***

131    A straight 4.5 m long reach of a perennial stream containing a single transverse knickpoint was  
132    selected for investigation on the west side of the ablation zone, ~ 0.85 km from the terminus  
133    (Figure 1). Glaciologically, perennial streams are channels that persist and are repeatedly  
134    reoccupied over inter-annual timescales, in contrast to annual streams that form and melt out  
135    each year (Ewing 1970). Perennial streams, especially on non-temperate glaciers, can seed the  
136    formation of englacial channels existing at atmospheric pressure (Gulley et al. 2009), therefore,  
137    providing a better analogue for englacial drainage than annual streams. Here, the selected reach  
138    was chosen for the presence of a knickpoint in isolation, with the absence of any distinct  
139    elevation changes that may have influenced knickpoint evolution. This stream was a  
140    distributary, bifurcating from a main channel 9 m above the reach, and appeared to exploit the  
141    downglacier oriented longitudinal foliation. The reach had a low gradient ( $7^\circ$ ) and sinuosity  
142    (1.005), and ranged in width from 0.14 to 0.66 m. Despite evidence of several transverse clear  
143    ice bands cutting across the channel upstream of the knickpoint, there was negligible transverse  
144    structural variability at, or downstream of the knickpoint, suggestive of a homogenous substrate  
145    underlying the step itself, allowing patterns and rates of change to be attributed to  
146    hydrodynamic variables. Although clastic debris was visible embedded in the channel bed  
147    (Figure 1B), the stream flow was devoid of sediment bed load, with little to no transportation  
148    of ice crystals over the measurement period.

149        The knickpoint was classified as a ‘break-in-gradient’ knickpoint type (after Haviv et  
150    al. 2010), characterised by a gentle step lip and riser face with a channel-bed-supported sloping  
151    jet (Figure 1C). Over the measurement period, this knickpoint accounted for between 15 and  
152    32 % of the 0.68 m decrease in elevation along the longitudinal profile of the stream reach.  
153    Initially, no pooling of water at the step base was observed; instead, a reverse bed slope was

154 recorded downstream of the knickpoint with detachment of flow from the channel bed and  
155 water aeration at the downstream end of this reverse slope.

156 [Figure 1 near here]

### 157 **3. Methods**

158 Data was collected in the early ablation season, between, and inclusive of, the 6<sup>th</sup> and 9<sup>th</sup> July  
159 2017. This short measurement period arose from considerable water flow reduction over the  
160 knickpoint on the 9<sup>th</sup> July, as a result of upstream flow capture. Knickpoint and channel  
161 cross-section measurements were completed between 08:00 and 12:00 before peak diurnal  
162 discharge, with the exception of the 6<sup>th</sup> July when measurements were taken between 14:00  
163 and 15:30 and excluded cross-section geometry. Using the assumption that peak discharge has  
164 the greatest impact on changing channel morphology (Marston 1983; Carver et al. 1994),  
165 geometric measurements are considered to reflect adjustments resulting from the previous  
166 day's hydrodynamic forcing. Adjustment was assessed between each day's measurements,  
167 giving three full days of change monitoring.

#### 168 **3.1 *Knickpoint and channel geometry***

169 To measure knickpoint geometry, the majority of water flow over the step was temporarily  
170 diverted to the main channel upstream of the reach, using sealed water-filled bags stacked at  
171 the distributary diffluence. Water flow was diverted for ~ 20 minutes each day between 08:50  
172 and 09:30. Once achieved, the horizontal distance of the step lip from a fixed reference point  
173 was measured to determine upstream knickpoint recession. Daily central longitudinal profiles  
174 of the step-riser were recorded using a contour gauge shaping tool, similar to techniques used  
175 for quantifying surface roughness (McCarroll and Nesje 1996). The gauge maintains the shape  
176 of a surface once moulded to it, allowing for replication with a quantified accuracy of 11 mm.  
177 Careful gauge positioning onto laminated millimetre graph paper enabled tracing of the



178 lowermost edge using a whiteboard marker pen, with nadir photography using a 14-mpx  
 179 Fujifilm Finepix JV200 digital camera allowing for extraction of profile coordinates. These  
 180 profile coordinates were digitally plotted at centimetre resolution, using a Bezier spline  
 181 interpolation to represent the step-riser (accurate to 5 mm).

182 Channel cross-section geometry was measured upstream and downstream of the  
 183 knickpoint lip, to quantify vertical incision (Figure 1). Measurements were conducted from  
 184 fixed reference points, established on the east stream bank. From these points, vertical depth  
 185 measurements to the nearest 10 mm were recorded at 0.1 m intervals across the channel,  
 186 relative to a taut tape measure anchored on the opposite bank. Vertical depth measurements  
 187 and the 0.1 m measurement intervals were trigonometrically corrected to a horizontal plane,  
 188 using the tape angle measured with a compass clinometer to  $\pm 1^\circ$ , with depth adjustment to the  
 189 daily glacier surface elevation. The inevitable tape sag led to an uncertainty ( $C_{\text{catenary}}$ ) that  
 190 was quantified following Uren and Price (2005):

$$191 \quad C_{\text{catenary}} = \frac{w^2 D^3 (\cos 2\theta)}{24T^2}$$

192 (Equation 1)

193 where  $w$  is weight per unit length of tape,  $D$  is tape length,  $\theta$  is the vertical angle between  
 194 end-points and  $T$  is applied tension. Assuming modest tension of 10 N, (following Irvine-Fynn  
 195 et al. (2014a)), for a tape length of 1.8 m and weight per unit length of  $0.18 \text{ N m}^{-1}$ , the maximum  
 196 uncertainty was 1 mm. Within the horizontal plane, inevitable positional uncertainty in repeat  
 197 surveys arises from ablation at the fixed reference points; however, this error is acceptable here,  
 198 as cross-sections are not directly compared in absolute space.

199 Bank full stage is unlikely within perennial supraglacial streams, as their existence  
 200 depends on incision outpacing ablation, at least initially (Knighton 1981; Marston 1983).

201 Therefore, flow geometry dimensions of the ‘active channel’ (width, mean channel depth  
 202 below the ice surface) were derived using water height at the channel thalweg (stage) at 10:00.  
 203 This ‘active channel’ denotes the area that adjusts in relation to actively flowing water  
 204 (Osterkamp and Hedman 1977), providing the best approximation of channel dimensions when  
 205 the channel is most stable prior to peak discharge. Daily incision rates were determined using  
 206 the difference between mean cross-section depths.

### 207 3.2 *Streamflow dynamics*

208 Stream discharge was measured at hourly intervals between 09:30 and 13:30. Following  
 209 Hudson and Fraser (2002), discharge ( $Q$ ) was estimated using salt dilution gauging:

210

$$211 \quad Q = \frac{k M}{(T_2 - T_1) \times (EC - EC_{bkgd})}$$

212

(Equation 2)

213 where  $M$  is mass of salt added in grams (here, 10 g pre-dissolved salt injected 11 m upstream  
 214 of the detection point);  $T_2 - T_1$  is tracer passage duration in seconds;  $EC - EC_{bkgd}$  is mean  
 215 electrical conductivity during the tracer passage, as measured with a REED SD-4307  
 216 conductivity meter (0.1  $\mu$ S resolution, accurate to  $\pm 2$  % (REED 2015)); and  $k$  is the  
 217 temperature-corrected proportionality constant, calculated as 1.5909 for 0 °C. Over the  
 218 observed temperature range of 0.01 – 0.3 °C, variation in  $k$  was less than 1 % and negligible  
 219 for discharge calculations. Measurements characterised the rising limb and beginning of the  
 220 falling limb of diurnal discharge and, thus, captured daily peak discharge between 11:30 and  
 221 12:30. An additional discharge reading was taken on the 6<sup>th</sup> July at 15:00, while it was not  
 222 possible to derive discharge on the 9<sup>th</sup> July, as flow was too low to measure.

223 Flow velocity along the reach was calculated from the salt tracer travel time over the  
224 thalweg distance and, following Knighton (1998), used with measurements of stage and flow  
225 width to calculate Froude and Reynolds numbers ( $Fr$  and  $Re$ , respectively). Daily maximum  
226 stream power per unit length over the knickpoint was estimated using the mean step gradient  
227 and peak discharge. Detailed observations were also made regarding the nature of water flow  
228 over the knickpoint, including defining the contact between the water and step-riser and  
229 evidence of hydraulic jumps, backpooling and splashing of water in relation to the channel  
230 morphology.

### 231 **3.3 Meteorological data**

232 In the absence of meteorological data at the glacier surface, hourly air temperature data over  
233 the measurement period were obtained from the nearest MeteoSwiss automatic weather station,  
234 located in Vicosoprano, 7 km from Vadrec del Forno. To interpolate these data to the local air  
235 temperature at the study site, a relationship describing the lapse rate between Vicosoprano and  
236 Vadrec del Forno was used, based on data from a HOBOware<sup>®</sup> weather station that had been  
237 installed on the ice during July 2016. The calculated lapse rate ( $r^2 = 0.72$ ,  $p \leq 0.01$ )  
238 was  $-0.009 \text{ }^\circ\text{C m}^{-1}$ , giving a difference of  $10.85 \text{ }^\circ\text{C}$  between the sites that was used to adjust the  
239 2017 air temperature data. Hourly potential incident radiation at the glacier surface was  
240 calculated following Irvine-Fynn et al. (2014b).

## 241 **4. Results**

### 242 **4.1 Knickpoint evolution**

243 The step lip migrated upstream by 0.26 m over three days from its initial 6<sup>th</sup> July position  
244 (Figure 2), with the step-riser face steepening by  $17^\circ$ . Knickpoint recession rates were variable,  
245 increasing from  $0.01 \text{ m day}^{-1}$  (6<sup>th</sup> - 7<sup>th</sup> July) to  $0.08 \text{ m day}^{-1}$  (7<sup>th</sup> - 8<sup>th</sup> July), with the greatest

246 recession of  $0.17 \text{ m day}^{-1}$  occurring between the 8<sup>th</sup> and 9<sup>th</sup> July, coincident with the greatest  
247 change in step gradient (Table 1).

248 Step height increased by 115 mm with the greatest change of 88 mm occurring between  
249 the 7<sup>th</sup> and 8<sup>th</sup> July. Between the 8<sup>th</sup> and 9<sup>th</sup> July, step height decreased by 18 mm. The reverse  
250 bed slope at the step base was replaced with the formation of a pool towards midday on the 8<sup>th</sup>  
251 July, with evidence of a hydraulic jump and backpooling.

252 [Figure 2 near here]

253 [Table 1 near here]

#### 254 **4.2 Cross-section evolution**

255 Measured cross-sections (Figure 3) show that above the knickpoint, the channel was generally  
256 wider and shallower than below the knickpoint. Over the measurement period, mean channel  
257 depth above the knickpoint was 0.40 m, and 0.52 m below the knickpoint. The nature and rates  
258 of morphological change were variable over both space and time, with disparity between the  
259 cross-sections. Above the knickpoint, the channel cross-section was initially approximately  
260 trapezoidal (Figure 3A; 7<sup>th</sup> July). This cross-section incised by 27 mm, developing a more  
261 rounded, quasi-elliptical morphology (Figure 3A; 8<sup>th</sup> July), which further incised by 83 mm  
262 and narrowed by 160 mm to form a more triangular morphology (Figure 3A; 9<sup>th</sup> July). Below  
263 the knickpoint (Figure 3B), the channel maintained an approximately triangular cross-section,  
264 with a stable width (Table 1) and incision of 73 mm over the first two days (6<sup>th</sup> - 7<sup>th</sup>, 7<sup>th</sup> - 8<sup>th</sup>  
265 July). This profile subsequently widened by 80 mm and incised by 20 mm (8<sup>th</sup> - 9<sup>th</sup> July).

266 The channel upstream of the knickpoint incised 18 mm more than that below, with the  
267 majority of vertical incision occurring between the 8<sup>th</sup> and 9<sup>th</sup> July above the step, and between  
268 the 7<sup>th</sup> and 8<sup>th</sup> July below the step (Table 1; cross-section mean depths). However, the greatest  
269 change in width was recorded between the 8<sup>th</sup> and 9<sup>th</sup> July for both cross-sections. As a result,

270 deepening and narrowing of the upstream cross-section coincided with a decrease in incision  
271 and widening of the downstream cross-section.

272 [Figure 3 near here]

### 273 4.3 *Streamflow dynamics*

274 Over the measurement period, discharge generally decreased (Table 1), with peak discharge on  
275 the 8<sup>th</sup> July being an order of magnitude lower than on previous days, and water flow on the 9<sup>th</sup>  
276 July being too low to measure. Water temperatures correlated positively with discharge  
277 ( $r = 0.83$ ,  $n = 11$ ,  $p \leq 0.01$ ). Expectedly, discharge also correlated positively with velocity  
278 ( $r = 0.82$ ,  $n = 11$ ,  $p \leq 0.01$ ) and stream power ( $r = 0.99$ ,  $n = 11$ ,  $p < 0.01$ ) and, thus, stream  
279 power was significantly lower on the 8<sup>th</sup> July than on previous days ( $p \leq 0.01$ ). The reduced  
280 discharge (8<sup>th</sup> and 9<sup>th</sup> July) was the result of upstream water capture, due to the main channel  
281 incising at a faster rate than the studied distributary reach. However, linear regressions between  
282 discharge and stream power with knickpoint retreat were not significant ( $p > 0.05$ ).

283 Water flow over the knickpoint was continuously channel-bed-supported, with only  
284 occasional observations of decoupled flow for a few seconds at a time. Water flow above and  
285 below the knickpoint was mainly subcritical ( $Fr < 1$ ) and was predominantly turbulent on the  
286 6<sup>th</sup> and 7<sup>th</sup> July (high  $Re$ ), with transitional flow on the 8<sup>th</sup> July (Table 1). As water neared the  
287 step base, lateral flow interaction with the channel banks resulted in water being diverted  
288 upwards and back towards the channel centre, causing flow convergence here and at the  
289 beginning of the reverse bed slope. A submerged impinging jet was observed at the step base.  
290 Downstream of the knickpoint, flow detachment from the channel bed occurred as the reverse  
291 bed slope deflected water upward, causing visible aeration and spraying of the channel banks.  
292 Immediately prior to midday on the 8<sup>th</sup> July, the effects of the reverse bed slope were less  
293 obvious and a hydraulic jump was present at the step base, with evidence of backpooling.

## 294 5. Discussion

### 295 5.1 *Hydrodynamic forcing*

296 In the absence of an appreciable bed load, it is reasonable to assume that erosive forces are  
297 predominantly hydrodynamic, with hydraulic action and melting driving supraglacial channel  
298 change (Knighton 1981; Marston 1983; Kostrzewski and Zwoliński 1995; Isenko et al. 2005).  
299 However, the results demonstrate that increased retreat rate was not associated with rising  
300 discharge and stream power per unit length. This supports suggestions that the relationship  
301 between discharge and knickpoint retreat rate is oversimplified (Baynes et al. 2018). Instead,  
302 the results here show that greater knickpoint retreat occurred at lower discharges. The changing  
303 step morphology indicates non-uniformity of erosion across the step, demonstrating the  
304 complex interaction between discharge regime and knickpoint evolution (see Section 5.2).  
305 Additionally, these data further demonstrate that the simplistic stream power incision model is  
306 unlikely to adequately characterise retreating knickpoints (Howard et al. 1994; Scheingross  
307 and Lamb 2017). This supports the work of St Germain and Moorman (2016), which  
308 demonstrated that supraglacial step-pool morphologies do not necessarily form at high  
309 discharge, contrary to assumptions by Vatne and Refsnes (2003) who regard high discharge as  
310 a necessary factor for step formation in ice. Furthermore, this challenges the assumption that  
311 the greatest channel change occurs at peak discharges in ice-walled channels (Marston 1983;  
312 Carver et al. 1994), highlighting the need for measurements at increased temporal resolution to  
313 better constrain the timing and rates of evolution.

314 As erosion reflects the balance between driving and resisting forces (Wohl 1998;  
315 Hayakawa and Matsukura 2003), the role of ice substrate resistance in controlling knickpoint  
316 migration rates must also be considered. The channel substrate comprised clear and bubbly ice  
317 types, the former of which experiences preferential water erosion (Ewing 1970; Hambrey  
318 1977), as exemplified by the undulating bed form troughs concordant with clear ice structures

319 upstream of the knickpoint (Figure 1B). The observed alternation in ice types through these  
320 bed forms, had they extended downstream, could have explained the relative stability of the  
321 step lip between the 6<sup>th</sup> and 7<sup>th</sup> July, with the subsequent increase in retreat rate being the result  
322 of headward migration through clear ice to less resistant, bubbly ice upstream. However, the  
323 absence of such structural features proximate to the knickpoint indicated a homogenous  
324 substrate here, reflected by knickpoint migration via replacement. This implies that knickpoint  
325 evolution was not structurally controlled during the measurement period, supporting the  
326 argument that hydrodynamic forcing plays the dominant role in governing supraglacial step  
327 evolution.

328         Within an ice-walled channel, thermal erosion is an additional contributing driver of  
329 knickpoint retreat. Such heat energy transfer arises from several sources: sensible air  
330 temperature and solar radiation, friction at the water-ice interface and turbulence-induced  
331 friction within the water (Ewing 1970; Ferguson 1973; Marston 1983). Additional erosion can  
332 arise from direct channel bed ablation through shallow water columns (Holmes 1955; Dozier  
333 1974). Although direct ablation may have been possible in this study, given the maximum  
334 recorded water depth of 0.1 m, this is not supported by the insignificant linear regression  
335 between daily mean potential incident radiation and incision rates ( $r = 0.027$ ,  $p > 0.05$ ). Using  
336 the 'Enter method', a multiple linear regression ( $R^2 = 0.62$ ) demonstrates that discharge was  
337 the only significant predictor of water temperature ( $r = 0.75$ ,  $p < 0.05$ ). This indicates that  
338 frictional heat generated from viscous flow dissipation is the main component of thermal  
339 erosion in this study, supporting research by Ferguson (1973), Parker (1975) and Marston  
340 (1983) who estimated that this can account for 50 – 75 % of incision. The overall slope of the  
341 stream reach here was 7°, with that of the knickpoint face being a minimum of 18°. As Pinchack  
342 (1972) reported a requisite channel gradient of 11° to induce melt in a slightly wider stream

343 than reported here, this indicates that frictional heat potentially plays more of a role in erosion  
344 locally, thereby contributing to knickpoint evolution.

## 345 **5.2 *Hydrological controls on supraglacial knickpoint evolution***

346 The notion that knickpoint retreat rate is primarily controlled by discharge (Seidl and Dietrich  
347 1992; Howard et al. 1994; Bishop et al. 2005) is challenged by the supraglacial stream data  
348 presented here. The greatest step retreat, gradient change and rate of upstream incision  
349 (Cross-section A) were associated with low discharges, and the greatest increase in step height  
350 and rate of downstream incision (Cross-section B) were associated with high discharges. To  
351 explain these spatial and temporal variations, we propose a conceptual model of  
352 process-morphology linkages to identify the hydrological controls on supraglacial knickpoint  
353 evolution, whereby varying discharge regimes control spatial zones of erosion over the  
354 step-riser and lead to pool formation (Figure 4). Three morphologically distinct zones of  
355 erosion are identified, with differential rates and magnitudes of change at the step lip, riser face  
356 and step base giving rise to knickpoint evolution via replacement of step morphology (Gardner  
357 1983).

358 At turbulent, high discharges, (here, 6<sup>th</sup> and 7<sup>th</sup> July), vertical incision is focused at the  
359 step base. The reduced boundary resistance at high flows means that the impinging jet retains  
360 energy over the step lip and face (Marston 1983; Wilcox and Wohl 2006; Comiti et al. 2009),  
361 therefore, imparting greater hydraulic force to the step base. However, as the channel bed and  
362 step face were not smoothly polished, channel roughness elements were limited to microscale  
363 features, indicating that reduced boundary resistance is likely to have a negligible impact on  
364 energy retention. At the step base, higher water temperatures associated with turbulence are  
365 more likely to contribute to vertical incision, aided by the high degree of interaction between  
366 the water jet and the channel bed. Incision rates at the step base exceed those at the lip, leading



367 to an increase in step height. Consequently, the knickpoint experiences considerable  
368 steepening, which contradicts the more often observed backward rotation of the knickpoint in  
369 homogenous bedrock and alluvial settings (Holland and Pickup 1976; Gardner 1983; Stein and  
370 Julien 1993; Frankel et al. 2007).

371 [Figure 4 near here]

372 At low discharges with transitional flow, (here, 8<sup>th</sup> and 9<sup>th</sup> July), erosion is focused on  
373 the reach immediately upstream of the knickpoint, the step lip and the step-riser face. At low  
374 water depths, the microscale channel roughness has a greater influence on frictional energy  
375 dissipation, increasing boundary resistance and resulting in accelerated melting of the bed  
376 upstream of the step, and at the step lip where shear stress is highest (Gardner 1983). The lower  
377 velocities associated with lower discharges act to increase the energy transfer time and, thus,  
378 enhance melt at a given point (Thorsness and Hanratty 1979), with low turbulence inhibiting  
379 energy dissipation within the flow itself. This occurs mainly above the step lip, where water  
380 flow is slower than across the step-riser as a result of the gentler slope. Additionally, enhanced  
381 erosion above the step lip is attributed to over-steepening (drawdown) of the water surface  
382 profile as flow starts to accelerate over the increasing gradient (Gardner 1983; Haviv et al.  
383 2006; Berlin and Anderson 2009). This enhanced energy transfer reduces the stream power of  
384 the bed-supported jet (Chin 2003), resulting in less available energy to hydraulically erode the  
385 step base and causing a decrease in step height.

386 The finding that low discharge has a dominant control on knickpoint migration  
387 necessitates consideration of the potential methodological impact of temporary stream  
388 diversion during low flows. The magnitude of knickpoint and channel adjustment was in the  
389 order of centimetres to decimetres over 24 hours, with peak diurnal discharge only exceeding  
390  $0.009 \text{ m}^3 \text{ s}^{-1}$  for a maximum of 3.5 hours over the measurement period. Low flow conditions  
391 of  $< 0.007 \text{ m}^3 \text{ s}^{-1}$  were recorded throughout the rest of the day, with flow diversion for 20

392 minutes accounting for < 2 % of this time, assuming continuous 24 hour flow. Consequently,  
393 we suggest that flow diversion over such a short period had negligible impact on knickpoint  
394 evolution; however, a portion of low flow channel adjustment may have been overlooked,  
395 albeit small, as a result of this diversion. The estimated maximum discharge diverted to the  
396 main channel ( $\sim 0.005 \text{ m}^3 \text{ s}^{-1}$ ) is not expected to have resulted in a marked change in incision  
397 rate or eventual channel capture over the timescales involved.

### 398 *5.2.1 Hydrological controls on pool development*

399 The lack of ice structural control over observed knickpoint evolution suggests that downstream  
400 pool development on the 8<sup>th</sup> July was primarily controlled by step morphology adjustment in  
401 response to discharge variations. Using the conceptual model described in Figure 4, an  
402 explanation for pool formation can be proposed. At high discharges, localised erosion at the  
403 step base leads to over-deepening. Water pools in this depression at low discharges, with the  
404 reverse bed slope acting to further impede downstream flow. As pool development starts to  
405 reduce the effect of the impinging jet on the channel bed (Wu and Rajaratnam 1998;  
406 Zimmermann and Church 2001; Carling et al. 2005), the increased tailwater depth inhibits  
407 vertical incision and results in a predominance of lateral erosion. In our study, this is  
408 demonstrated by the coincident decrease in channel depth and increase in width below the  
409 knickpoint between the 8<sup>th</sup> and 9<sup>th</sup> July. The pooled water creates a persistent contact with the  
410 ice forming the lower section of the step-riser, causing erosion here (Figure 4), and resulting in  
411 continued and accelerated steepening of the face at low discharge. Turbulent secondary  
412 circulation back towards the step face and the formation of a hydraulic jump close to the step  
413 base enhances this erosional zone. Pool development herein appears to conform  
414 morphologically to the conceptual model proposed by Scheingross et al. (2017) to describe  
415 abrasive plunge-pool evolution in homogenous bedrock. This suggests that in a homogenous

416 ice substrate and, even in the absence of sediment load, knickpoint retreat may be driven by  
417 vertical drilling, a knickpoint migration process described by Howard et al. (1994) and Lamb  
418 et al. (2007). This contrasts with classic waterfall erosion models that indicate knickpoint  
419 migration owing to overlying caprock failure, following removal of an underlying substrate  
420 (e.g. Gilbert 1890; Holland and Pickup 1976; Frankel et al. 2007). However, the lack of  
421 undercutting herein may be due to the reduced discharge following pool formation, with  
422 accelerated erosion of the upstream pool wall only being plausible in the case of continued  
423 flow.

424         Although substrate characteristics influence the shape and recession rate of knickpoints  
425 (Gardner 1983; Larue 2008; Phillips and Desloges 2014), our proposed model builds on the  
426 concept that a mutual interaction exists between the shape of the heat transfer surface and the  
427 variation in rates of heat transfer, the latter of which is determined by flow characteristics  
428 (Gilpin et al. 1980). This advances the work of Vatne and Irvine-Fynn (2016), whose insights  
429 from englacial knickpoint morphology indicated that step shape controls the type of water jet  
430 and, thus, the location of energy expenditure and heat transfer across the knickpoint face. Our  
431 model demonstrates that differing discharge regimes govern the location of erosion, a concept  
432 that can be extended to knickpoint evolution in bedrock (Carling et al. 2005) and cohesive  
433 sediment (Bennet et al. 2000), where varying degrees of surface erosion in relation to  
434 hydrological forcing have also been recorded. However, the difference in erosive mechanisms  
435 between supraglacial and bedrock/alluvial channels indicates that this model is not applicable  
436 within the latter for determining the ways in which knickpoint morphology will adjust in  
437 response to discharge alterations. Contrary to some previous assertions (e.g. Ewing 1970;  
438 Marston 1983; Knighton 1985), this shows that the systems are not analogous to one another,  
439 warranting further investigation into the differences between each environment and the  
440 processes causing the formation and adjustment of similar channel morphologies.

### 441        5.3    *Interactions between morphology and flow variability*

442    The zones of erosion outlined in Section 5.2 govern step and channel shape, and demonstrate  
443    the effect of flow dynamics on knickpoint morphology. However, channel morphology also  
444    controls flow dynamics over a step (e.g. Knighton 1981; Kostrzewski and Zwoliński 1995;  
445    Milzow et al. 2006), determining these erosional zones. Here, this is exemplified by channel  
446    narrowing over the knickpoint, confining water flow over the step-riser and resulting in water  
447    overturning towards the channel centre with consequent flow convergence. This, in turn, gives  
448    rise to the narrow cross-section at the step base, with water concentration driving vertical  
449    incision. This feedback between channel morphology and hydraulics is complex, making it  
450    difficult to identify clear cause-and-effect relationships (Wilcox et al. 2011).

451        In order to determine the importance of the erosional zones outlined here in controlling  
452    knickpoint morphology and recession rates, knickpoint evolution was modelled (Figure 5)  
453    using the daily ice melt rate as an equivalent erosional process for the stream power incision  
454    model. Channel incision rates were derived from daily mean water temperature and velocity,  
455    using relationships described in Isenko et al. (2005)'s Figure 2. Each knickpoint profile was  
456    divided into linear millimetre-to-centimetre length segments based on changes in gradient  
457    using Rhino3D<sup>®</sup> software (Robert McNeel & Associates 2017), with application of calculated  
458    daily incision rates perpendicular to the local slope of each segment. Perpendicular offsetting  
459    of each segment reflected changes in the horizontal and vertical plane, and better characterised  
460    knickpoint retreat and morphological adjustment. A manually digitised curve joined the offset  
461    segments to create a full modelled profile (Figure 5). As discharge prior to 08:00 was  
462    consistently low ( $< 0.005 \text{ m}^3 \text{ s}^{-1}$ ), it is assumed that stream flow is also low in the evening and  
463    negligible overnight. This assumption is supported by the high snow line position in July 2017,  
464    akin to that typically seen in late summer (Beat Kühnis, personal communication, July 2017).  
465    Snowpack depletion reduces potential water storage at the glacier surface, the volume of

466 delayed runoff and the lag-time between peak melt and supraglacial discharge (see Willis et al.  
467 2002). Here, the contribution of delayed runoff following peak ablation is likely to be minimal,  
468 indicating that the stream did not experience continuous water flow over a 24-hour period.  
469 Therefore, incision rates were applied for an 18-hour period to represent a maximum estimate  
470 of change, as the mean water temperatures and velocities used encompassed the rising limb  
471 and peak diurnal measurements.

472 [Figure 5 near here]

473         Comparison of the modelled profiles with observed knickpoint evolution emphasise  
474 discrepancies between both the shape and rate of evolution (Figure 5). Modelled profiles  
475 retained the original step morphology, overestimating vertical lowering (6<sup>th</sup> - 7<sup>th</sup>, 8<sup>th</sup> - 9<sup>th</sup> July)  
476 and both overestimating (6<sup>th</sup> - 7<sup>th</sup> July) and underestimating headward recession at the step lip  
477 (7<sup>th</sup> - 8<sup>th</sup>, 8<sup>th</sup> - 9<sup>th</sup> July). The inability of the model to accurately predict knickpoint evolution on  
478 ice is likely due to the assumption of constant water temperature and velocity along the profile.  
479 As the results herein demonstrate that differential zones of erosion arise at differing discharges,  
480 this suggests that use of a constant-rate melt model for characterising step evolution is too  
481 simplistic, similar to the stream power laws applied in bedrock/alluvial streams. The  
482 complexities of changing flow dynamics across a knickpoint on ice must be further  
483 investigated, to allow incorporation of these parameters and their feedback with the channel  
484 boundary into numerical models.

## 485         **6. Conclusions**

486         Until now, there has been a limited process-level understanding of knickpoint evolution within  
487 ice-walled channels, despite their importance in supraglacial and englacial incision processes.  
488         Our study of a supraglacial knickpoint on Vadrec del Forno, Switzerland provides the first  
489 detailed dataset of supraglacial knickpoint morphological change at a fine temporal resolution.  
490         The results showed recession of 0.26 m over three days, with variable rates and magnitudes of

491 change, both spatially across the knickpoint and temporally over diurnal timescales. Low flow  
492 rates coincided with the greatest step retreat, gradient change and rate of upstream incision,  
493 and high flow rates coincided with the greatest increase in step height and rate of downstream  
494 incision. Our conceptual model proposes that discharge variations control the zones of erosion  
495 over the knickpoint, with low discharge focusing erosion on the reach upstream of the  
496 knickpoint, the step lip and step-riser face, and high discharge focusing erosion at the  
497 knickpoint base. Channel over-deepening at the knickpoint base led to pool formation, with the  
498 increased tailwater depth inhibiting vertical incision and causing lateral erosion. This confirms  
499 non-uniform water flow over the step, resulting in evolution through replacement of  
500 morphology. Bed load absence within the stream indicates the hydrodynamic nature of  
501 evolution, with the driving forces of hydraulic action and frictional thermal erosion governing  
502 morphological change. The results indicate that peak discharge may not play as dominant a  
503 role in drainage development on ice as previously considered, suggesting that the majority of  
504 morphological adjustment in features such as knickpoints may occur prior to or following high  
505 meltwater fluxes, either at a diurnal (supraglacial) or seasonal (englacial) scale.

506         The data presented here demonstrate that the relationships between discharge, stream  
507 power and knickpoint retreat rate commonly used in bedrock/alluvial channels fails to capture  
508 the intricacies and feedbacks of erosion processes driving knickpoint recession in ice-walled  
509 channels. Our findings show that the considerable differences in erosive mechanisms between  
510 supraglacial and bedrock/alluvial channels are likely to result in disparities in knickpoint  
511 morphological adjustment in response to varying discharge regimes. The conceptual model  
512 proposed herein has been developed from a relatively time-limited dataset, meaning that  
513 ascertaining whether results provide a relevant representation of knickpoint evolution is  
514 challenging. In order to test the wider application of the model, additional research within  
515 supraglacial environments is required at a range of spatial scales, taking into consideration

516 channels of varying sizes, gradients and discharges. In particular, further investigation of  
517 knickpoint erosion mechanisms in relation to variable flow regimes is essential, through  
518 increasing the *temporal* and *spatial* resolution of flow measurements above, across and below  
519 knickpoints.

## 520 **Acknowledgements**

521 This work was supported by a Knowledge Economy Skills Scholarship (KESS II) under Project  
522 AU10003, a pan-Wales higher-level skills initiative led by Bangor University on behalf of the HE sector  
523 in Wales. It is part-funded by the Welsh Government's European Social Fund (ESF) convergence  
524 programme for West Wales and the Valleys. Funding was awarded to TDLI-F and JEK, with support  
525 from Deri Jones & Associates Ltd. Additional support was gratefully received from the Aberystwyth  
526 University Research Fund "ASPECT" under Grant number 12104 awarded to TDLI-F, Aberystwyth  
527 University Research Fund under Grant number 12465 awarded to TOH and TDLI-F, and the Royal  
528 Geographical Society Small Research Grant under Grant number SRG8/16 awarded to TOH. All  
529 authors recognise additional support from Aberystwyth University (DGES). MeteoSwiss are  
530 acknowledged for the provision of automatic weather station data. Emily Stratton, Ed Roberts, Sarah  
531 Easter, Nathan Daverson and Charlotte Day are all thanked for their support in the field. Edwin Baynes  
532 is thanked for initial discussions regarding the research nature and data collection, and for an informal  
533 review of the original manuscript, and helpful comments were also gratefully received from Emily  
534 Parker. The constructive comments from two anonymous reviewers are gratefully acknowledged.

## 535 **Disclosure statement**

536 No potential conflict of interest was reported by the authors.

## 537 **Notes on contributors**

538 JEK is a PhD student in Glaciology at the Centre for Glaciology, Aberystwyth University. Her  
539 main area of research is glacier drainage morphology.

540 TDLI-F is a Senior Lecturer in Geography at Aberystwyth University. His main area of  
541 research is glacial hydrology, which includes the hydraulics of the near-surface ice, the  
542 seasonal development of ice surface roughness and albedo, and glacier surface microbial

543 processes.

544 TOH is a Lecturer in Geography at Aberystwyth University, specialising in glaciology and  
545 remote sensing. His research focuses on the use of optical, radar and microwave imagery and  
546 data to quantify changes in the cryosphere.

547 JPPJ is an engineering consultant and surveyor specialising in marine design and laser scanning  
548 for Deri Jones & Associates Ltd. His work focuses on the design of construction systems for  
549 large structures, and on capturing 3D information for complex man-made and natural  
550 structures.

551 ST is a Professor of Geography at Aberystwyth University. His main areas of research include  
552 fluvial geomorphology and sedimentology, with a particular focus on bedrock and alluvial  
553 rivers in drylands.

554 HMG is a Senior Lecturer in Geography at Aberystwyth University. His main areas of research  
555 include processes and rates of change in fluvial systems and reconstructing flood histories using  
556 geomorphological and documentary methods.

557 BH is a Professor of Geography at Aberystwyth University. His main areas of research include  
558 the links between subglacial drainage and ice motion, structural glaciology and glacier-like  
559 forms on Mars.

#### 560 **Author contributions**

561 JEK and TDLI-F developed the research question and context; JEK designed and conducted  
562 the research; JEK analysed and interpreted the data, and wrote the paper with guidance from  
563 TDLI-F; TOH provided UAV imagery of the field site. All authors edited and revised the paper.



564 **References**

- 565 Abrahams AD, Li G, Atkinson JF. 1995. Step-pool streams: Adjustment to maximum flow resistance.  
566 *Water Resour Res.* 31(10):2593-2602.
- 567 Baynes ER, Lague D, Attal M, Gangloff A, Kirstein LA, Dugmore AJ. 2018. River self-organisation  
568 inhibits discharge control on waterfall migration. *Sci Rep.* 8(1):2444.
- 569 Bennet SJ, Robinson KM, Simon A, Hanson GJ. 2000. Stable knickpoints formed in cohesive  
570 sediment. Joint Conference on Water Resource Engineering and Water Resources Planning and  
571 Management; 30th July - August 2nd; Minneapolis, MN.
- 572 Berlin MM, Anderson RS. 2007. Modeling of knickpoint retreat on the Roan Plateau, western  
573 Colorado. *J Geophys Res Earth Surf.* 112(F3).
- 574 Berlin MM, Anderson RS. 2009. Steepened channels upstream of knickpoints: Controls on relict  
575 landscape response. *J Geophys Res Earth Surf.* 114(F03018).
- 576 Bigi A, Hasbargen LE, Montanari A, Paola C. 2006. Knickpoints and hillslope failures: Interactions in  
577 a steady-state experimental landscape. *Special Papers Geological Society of America.* 398:295-307.
- 578 Bishop P, Hoey TB, Jansen JD, Artza IL. 2005. Knickpoint recession rate and catchment area: the  
579 case of uplifted rivers in Eastern Scotland. *Earth Surf Processes Landforms.* 30(6):767-778.
- 580 Brush JLM, Wolman GM. 1960. Knickpoint behavior in noncohesive material: a laboratory study.  
581 *Geol Soc Am Bull.* 71(1):59-74.
- 582 Brykala D. 1999. Hydraulic geometry of a supraglacial stream on the Waldemar Glacier (Spitsbergen)  
583 in the summer of 1997. *Polish Polar Studies: 26th International Polar Symposium; June 1999; Lublin,*  
584 *Poland.* p. 51-64.
- 585 Carling P, Tych W, Richardson K. 2005. The hydraulic scaling of step-pool systems. *River, Coastal*  
586 *and Estuarine Morphodynamics.* New York: Taylor & Francis; p. 55-63.
- 587 Carver S, Sear D, Valentine E. 1994. An observation of roll waves in a supraglacial meltwater  
588 channel, Harlech Gletscher, East Greenland. *J Glaciol.* 40(134):75-78.

- 589 Chartrand SM, Whiting PJ. 2000. Alluvial architecture in headwater streams with special emphasis on  
590 step-pool topography. *Earth Surf Processes Landforms*. 25(6):583-600.
- 591 Chin A. 2003. The geomorphic significance of step-pools in mountain streams. *Geomorphology*.  
592 55(1-4):125-137.
- 593 Comiti F, Cadol D, Wohl EE. 2009. Flow regimes, bed morphology, and flow resistance in self-  
594 formed step-pool channels. *Water Resour Res*. 45(4):W04424.
- 595 Cook KL, Turowski JM, Hovius N. 2013. A demonstration of the importance of bedload transport for  
596 fluvial bedrock erosion and knickpoint propagation. *Earth Surf Processes Landforms*. 38(7):683-695.
- 597 Crosby BT, Whipple KX. 2006. Knickpoint initiation and distribution within fluvial networks: 236  
598 waterfalls in the Waipaoa River, North Island, New Zealand. *Geomorphology*. 82(1-2):16-38.
- 599 Curran JH, Wohl EE. 2003. Large woody debris and flow resistance in step-pool channels, Cascade  
600 Range, Washington. *Geomorphology*. 51(1-3):141-157.
- 601 Dozier J. 1974. Channel adjustments in supraglacial streams. Icefield Ranges Research Project,  
602 Scientific Results. 4:189-205.
- 603 Dust D, Wohl E. 2012. Characterization of the hydraulics at natural step crests in step-pool streams  
604 via weir flow concepts. *Water Resour Res*. 48(W09542).
- 605 Ewing KJ. 1970. Supraglacial streams on the Kaskawulsh Glacier, Yukon Territory. *Arctic Institute of*  
606 *North America Research paper*. 57:121-167.
- 607 Ferguson RI. 1973. Sinuosity of supraglacial streams. *Geol Soc Am Bull*. 84(1):251-256.
- 608 Frankel KL, Pazzaglia FJ, Vaughn JD. 2007. Knickpoint evolution in a vertically bedded substrate,  
609 upstream-dipping terraces, and Atlantic slope bedrock channels. *Geol Soc Am Bull*. 119(3-4):476-  
610 486.
- 611 Gardner TW. 1983. Experimental study of knickpoint and longitudinal profile evolution in cohesive,  
612 homogenous material. *Geol Soc Am Bull*. 94(5):664-672.

- 613 Gilbert G. 1890. The history of the Niagara River: extracted from the sixth annual report to the  
614 Commissioners of the State Reservation at Niagara, for the year 1889. Albany, NY.
- 615 Gilpin R, Hirata T, Cheng K. 1980. Wave formation and heat transfer at an ice-water interface in the  
616 presence of a turbulent flow. *J Fluid Mech.* 99(3):619-640.
- 617 Gleason CJ, Smith LC, Chu VW, Legleiter CJ, Pitcher LH, Overstreet BT, Rennermalm AK, Forster  
618 RR, Yang K. 2016. Characterizing supraglacial meltwater channel hydraulics on the Greenland Ice  
619 Sheet from in situ observations. *Earth Surf Processes Landforms.* 41(14):2111-2122.
- 620 Grimaud J-L, Paola C, Voller V. 2015. Experimental migration of knickpoints: influence of style of  
621 base-level fall and bed lithology. *Earth Surf Dyn.* 3(3):11-23.
- 622 Griselin M. 1992. In the depth of a small polar glacier (Loven East Glacier, Spitsbergen). Proceedings  
623 of the 2nd International GLACKIPR Symposium; 10-16 February; University of Silesia, Poland. p.  
624 51-63.
- 625 Gulley JD, Benn DI, Müller D, Luckman A. 2009. A cut-and-closure origin for englacial conduits in  
626 uncrevassed regions of polythermal glaciers. *J Glaciol.* 55(189):66-80.
- 627 Hambrey MJ. 1977. Supraglacial drainage and its relationship to structure, with particular reference to  
628 Charles Rabots Bre, Okstindan, Norway. *Norsk Geografisk Tidsskrift.* 31(2):69-77.
- 629 Haviv I, Enzel Y, Whipple K, Zilberman E, Matmon A, Stone J, Fifield K. 2010. Evolution of vertical  
630 knickpoints (waterfalls) with resistant caprock: Insights from numerical modeling. *J Geophys Res F:*  
631 *Earth Surf.* 115(F03028).
- 632 Haviv I, Enzel Y, Whipple KX, Zilberman E, Stone J, Matmon A, Fifield LK. 2006. Amplified  
633 erosion above waterfalls and oversteepened bedrock reaches. *J Geophys Res F: Earth Surf.*  
634 111(F04004).
- 635 Hayakawa Y, Matsukura Y. 2003. Recession rates of waterfalls in Boso Peninsula, Japan, and a  
636 predictive equation. *Earth Surf Processes Landforms.* 28(6):675-684.
- 637 Holland W, Pickup G. 1976. Flume study of knickpoint development in stratified sediment. *Geol Soc*  
638 *Am Bull.* 87(1):76-82.

- 639 Holmes GW. 1955. Morphology and hydrology of the Mint Julep area, Southwest Greenland.  
640 Alabama, US: Air University. Mint Julep Reports., Part II: A-104-B.
- 641 Holmlund P. 1988. Internal geometry and evolution of moulins, Storglaciären, Sweden. *J Glaciol.*  
642 34(117):242-248.
- 643 Howard AD, Dietrich WE, Seidl MA. 1994. Modeling fluvial erosion on regional to continental  
644 scales. *J Geophys Res B: Solid Earth.* 99(B7):13971-13986.
- 645 Hudson R, Fraser J. 2002. Alternative methods of flow rating in small coastal streams. BC, Canada:  
646 Forest Service British Columbia. EN-014.
- 647 Irvine-Fynn TDL, Sanz-Ablanedo E, Rutter N, Smith MW, Chandler JH. 2014a. Measuring glacier  
648 surface roughness using plot-scale, close-range digital photogrammetry. *J Glaciol.* 60(223):957-969.
- 649 Irvine-Fynn TDL, Hanna E, Barrand N, Porter P, Kohler J, Hodson A. 2014b. Examination of a  
650 physically based, high-resolution, distributed Arctic temperature-index melt model, on Midtre  
651 Lovénbreen, Svalbard. *Hydrol Processes.* 28(1):134-149.
- 652 Isenko E, Naruse R, Mavlyudov B. 2005. Water temperature in englacial and supraglacial channels:  
653 Change along the flow and contribution to ice melting on the channel wall. *Cold Reg Sci Technol.*  
654 42(1):53-62.
- 655 Jansen JD, Fabel D, Bishop P, Xu S, Schnabel C, Codilean AT. 2011. Does decreasing paraglacial  
656 sediment supply slow knickpoint retreat? *Geology.* 39(6):543-546.
- 657 Jennings SJ, Hambrey MJ, Glasser NF. 2014. Ice flow-unit influence on glacier structure, debris  
658 entrainment and transport. *Earth Surf Processes Landforms.* 39(10):1279-1292.
- 659 Joughin I, Das SB, Flowers G, Behn MD, Alley RB, King MA, Smith B, Bamber JL, van den Broeke  
660 MR, Van Angelen J. 2013. Influence of ice-sheet geometry and supraglacial lakes on seasonal ice-  
661 flow variability. *The Cryosphere.* 7(4):1185-1192.
- 662 Karlstrom L, Gajjar P, Manga M. 2013. Meander formation in supraglacial streams. *J Geophys Res*  
663 *Earth Surf.* 118(3):1897-1907.

- 664 Karlstrom L, Yang K. 2016. Fluvial supraglacial landscape evolution on the Greenland Ice Sheet.  
665 Geophys Res Lett. 43(6):2683-2692.
- 666 Kephart CW. 2013. Flow and geometry measurements at an active knickpoint [Master's thesis].  
667 Lincoln: University of Nebraska.
- 668 Knighton AD. 1972. Meandering habit of supraglacial streams. Geol Soc Am Bull. 83(1):201-204.
- 669 Knighton AD. 1981. Channel form and flow characteristics of supraglacial streams, Austre  
670 Okstindbreen, Norway. Arct Alp Res. 13(3):295-306.
- 671 Knighton AD. 1985. Channel form adjustment in supraglacial streams, Austre Okstindbreen, Norway.  
672 Arct Alp Res. 17(4):451-466.
- 673 Knighton AD. 1998. Fluvial Forms and Processes. London: Hodder Arnold.
- 674 Kostrzewski A, Zwoliński Z. 1995. Hydraulic geometry of a supraglacial stream. Quaestiones  
675 Geographicae. [accessed 11/05/2018]:[165-176 p.]. <http://www.staff.amu.edu.pl/~zbzw/gh/gh1.htm>.
- 676 Lague D. 2014. The stream power river incision model: evidence, theory and beyond. Earth Surf  
677 Processes Landforms. 39(1):38-61.
- 678 Lamb MP, Finnegan NJ, Scheingross JS, Sklar LS. 2015. New insights into the mechanics of fluvial  
679 bedrock erosion through flume experiments and theory. Geomorphology. 244:33-55.
- 680 Lamb MP, Howard AD, Dietrich WE, Perron JT. 2007. Formation of amphitheater-headed valleys by  
681 waterfall erosion after large-scale slumping on Hawai'i. Geol Soc Am Bull. 119(7-8):805-822.
- 682 Lampkin D, VanderBerg J. 2014. Supraglacial melt channel networks in the Jakobshavn Isbræ region  
683 during the 2007 melt season. Hydrol Processes. 28(25):6038-6053.
- 684 Larue J-P. 2008. Effects of tectonics and lithology on long profiles of 16 rivers of the southern Central  
685 Massif border between the Aude and the Orb (France). Geomorphology. 93(3-4):343-367.
- 686 Leopold LB, Bagnold RA, Wolman MG, Brush JLM. 1960. Flow resistance in sinuous or irregular  
687 channels. Washington, D.C.: Geological Survey Professional Paper. 282-D:111.

- 688 Mackey BH, Scheingross JS, Lamb MP, Farley KA. 2014. Knickpoint formation, rapid propagation,  
689 and landscape response following coastal cliff retreat at the last interglacial sea-level highstand:  
690 Kaua'i, Hawai'i. *Geol Soc Am Bull.* 126(7-8):925-942.
- 691 Mantelli E, Camporeale C, Ridolfi L. 2015. Supraglacial channel inception: Modeling and processes.  
692 *Water Resour Res.* 51(9):7044-7063.
- 693 Marston RA. 1983. Supraglacial stream dynamics on the Juneau Icefield. *Ann Assoc Am Geogr.*  
694 73(4):597-608.
- 695 McCarroll D, Nesje A. 1996. Rock surface roughness as an indicator of degree of rock surface  
696 weathering. *Earth Surf Processes Landforms.* 21(10):963-977.
- 697 Milzow C, Molnar P, McArdell BW, Burlando P. 2006. Spatial organization in the step-pool structure  
698 of a steep mountain stream (Vogelbach, Switzerland). *Water Resour Res.* 42(W04418).
- 699 Osterkamp W, Hedman E. 1977. Variation of width and discharge for natural high-gradient stream  
700 channels. *Water Resour Res.* 13(2):256-258.
- 701 Park CC. 1981. Hydraulic geometry of a supraglacial stream: some observations from the Val  
702 d'herens, Switzerland. *Revue de Géomorphologie Dynamique.* 30(1):1-9.
- 703 Parker G. 1975. Meandering of supraglacial melt streams. *Water Resour Res.* 11(4):551-552.
- 704 Phillips JD, McCormack S, Duan J, Russo JP, Schumacher AM, Tripathi GN, Brockman RB, Mays  
705 AB, Pulugurtha S. 2010. Origin and interpretation of knickpoints in the Big South Fork River basin,  
706 Kentucky–Tennessee. *Geomorphology.* 114(3):188-198.
- 707 Phillips R, Desloges J. 2014. Glacially conditioned specific stream powers in low-relief river  
708 catchments of the southern Laurentian Great Lakes. *Geomorphology.* 206:271-287.
- 709 Piccini L, Romeo A, Badino G. 2002. Moulins and marginal contact caves in the Gornergletscher,  
710 Switzerland. *Nimbus.* 23-24:94-99.
- 711 Pinchack AC. 1972. Diurnal flow variations and thermal erosion in supraglacial streams. East  
712 Lansing, Michigan: Michigan State University. Technical Report 33: Part XII.

- 713 PlanetTeam. 2017. Planet Application Program Interface: In Space for Life on Earth. San Francisco,  
714 CA.
- 715 Pulina M. 1984. Glacierkarst phenomena in Spitsbergen. *Norsk Geografisk Tidsskrift*. 38(3-4):163-  
716 168.
- 717 REED Instruments. 2015. REED SD-4307 Salt/TDS/Conductivity Datalogger Instruction Manual.  
718 REED Instruments.
- 719 Rippin DM, Pomfret A, King N. 2015. High resolution mapping of supra-glacial drainage pathways  
720 reveals link between micro-channel drainage density, surface roughness and surface reflectance. *Earth  
721 Surf Processes Landforms*. 40(10):1279-1290.
- 722 Robert McNeel & Associates. 2017. Rhino3D software Version 5. Barcelona: Robert McNeel &  
723 Associates.
- 724 Scheingross JS, Lamb MP. 2017. A mechanistic model of waterfall plunge pool erosion into bedrock.  
725 *J Geophys Res F: Earth Surf*. 122(11):2079-2104.
- 726 Scheingross JS, Lo DY, Lamb MP. 2017. Self-formed waterfall plunge pools in homogeneous rock.  
727 *Geophys Res Lett*. 44(1):200-208.
- 728 Seidl M, Dietrich W. 1992. The problem of bedrock channel erosion. *Catena Supplement*. 23:101-  
729 124.
- 730 Smith LC, Chu VW, Yang K, Gleason CJ, Pitcher LH, Rennermalm AK, Legleiter CJ, Behar AE,  
731 Overstreet BT, Moustafa SE. 2015. Efficient meltwater drainage through supraglacial streams and  
732 rivers on the southwest Greenland Ice Sheet. *Proc Natl Acad Sci USA*. 112(4):1001-1006.
- 733 St Germain S, Moorman B. 2016. The development of a pulsating supraglacial stream. *Ann Glaciol*.  
734 57(72):31-38.
- 735 Stein O, Julien P. 1993. Criterion delineating the mode of headcut migration. *J Hydraul Eng*.  
736 119(1):37-50.
- 737 Thorsness C, Hanratty T. 1979. Mass-transfer between a flowing fluid and a solid wavy surface.  
738 *AIChE Journal*. 25(4):686-697.

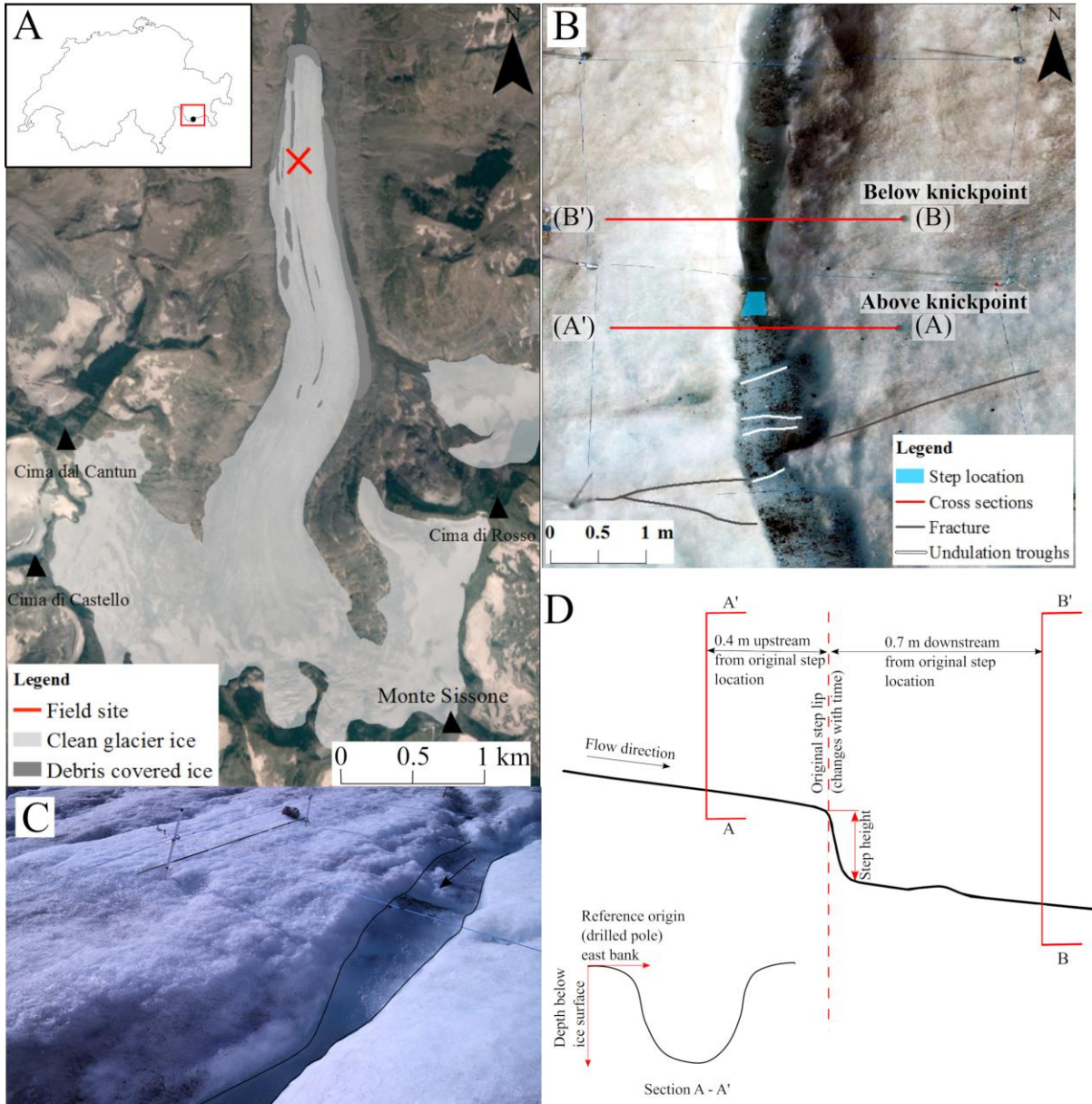
- 739 Tucker G, Whipple K. 2002. Topographic outcomes predicted by stream erosion models: Sensitivity  
740 analysis and intermodel comparison. *J Geophys Res B: Solid Earth*. 107(B9).
- 741 Uren J, Price W. 2005. *Surveying for engineers*. 4th ed. New York: Palgrave Macmillan.
- 742 Vatne G. 2001. Geometry of englacial water conduits, Austre Brøggerbreen, Svalbard. *Norsk*  
743 *Geografisk Tidsskrift*. 55(2):85-93.
- 744 Vatne G, Irvine-Fynn TDL. 2016. Morphological dynamics of an englacial channel. *Hydrol Earth*  
745 *Syst Sci*. 20(7):2947-2964.
- 746 Vatne G, Refsnes I. 2003. Channel pattern and geometry of englacial conduits. 6th International  
747 Symposium 'Glacier caves and karst in Polar Regions'; Ny-Ålesund, Svalbard. p. 181-188.
- 748 Whipple KX, Tucker GE. 1999. Dynamics of the stream-power river incision model: Implications for  
749 height limits of mountain ranges, landscape response timescales, and research needs. *J Geophys Res*  
750 *B: Solid Earth*. 104(B8):17661-17674.
- 751 Whittaker AC, Boulton SJ. 2012. Tectonic and climatic controls on knickpoint retreat rates and  
752 landscape response times. *J Geophys Res F: Earth Surf*. 117(F2).
- 753 Wilcox AC, Wohl EE. 2006. Flow resistance dynamics in step-pool stream channels: 1. Large woody  
754 debris and controls on total resistance. *Water Resour Res*. 42(5):W05418.
- 755 Wilcox AC, Wohl EE, Comiti F, Mao L. 2011. Hydraulics, morphology, and energy dissipation in an  
756 alpine step-pool channel. *Water Resour Res*. 47(7):W07514.
- 757 Willis IC, Arnold NS, Brock BW. 2002. Effect of snowpack removal on energy balance, melt and  
758 runoff in a small supraglacial catchment. *Hydrol Process*. 16(14):2721-2749.
- 759 Wohl EE. 1998. Bedrock channel morphology in relation to erosional processes. In: Tinkler KJ, Wohl  
760 EE, editors. *Rivers Over Rock: Fluvial Processes in Bedrock Channels*. Washington, D.C.: American  
761 Geophysical Union; p. 133-151.
- 762 Wu S, Rajaratnam N. 1998. Impinging jet and surface flow regimes at drop. *J Hydrol Res* 36(1):69-  
763 74.



- 764 Yang K, Smith LC, Chu VW, Pitcher LH, Gleason CJ, Rennermalm AK, Li M. 2016. Fluvial  
765 morphometry of supraglacial river networks on the southwest Greenland Ice Sheet. *GIScience &*  
766 *Remote Sensing*. 53(4):459-482.
- 767 Yokokawa M, Izumi N, Naito K, Parker G, Yamada T, Greve R. 2016. Cyclic steps on ice. *J Geophys*  
768 *Res Earth Surf*. 121(5):1023-1048.
- 769 Zimmermann A, Church M. 2001. Channel morphology, gradient profiles and bed stresses during  
770 flood in a step-pool channel. *Geomorphology*. 40(3-4):311-327.

771 **Table 1.** Summary of knickpoint and cross-section dimensions, flow parameters, and general interpolated weather trends for each day.

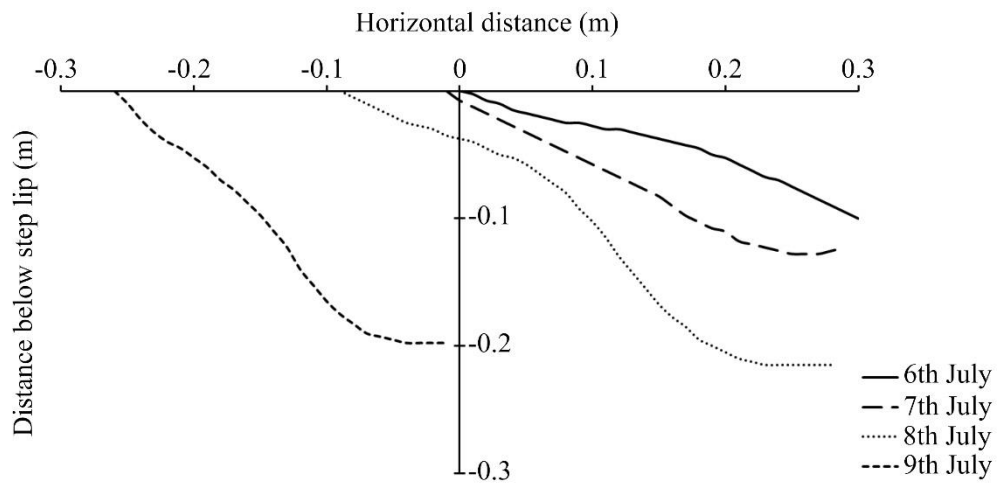
Day	Step height (mm)	Step gradient (°)	Cross-section above knickpoint		Cross-section below knickpoint		Peak discharge ( $\text{m}^3 \text{s}^{-1}$ )	Mean velocity ( $\text{m s}^{-1}$ )	Maximum stream power per unit length ( $\text{W m}^{-1}$ )	Mean water temperature ( $^{\circ}\text{C}$ )	Froude number range		Reynolds number range	Mean daily air temperature ( $^{\circ}\text{C}$ )	Mean daily potential incident radiation ( $\text{W m}^{-2}$ )
			Mean depth (m)	Width (m)	Mean depth (m)	Width (m)					Above knickpoint	Below knickpoint			
<b>6<sup>th</sup> July</b>	100	18	-	-	-	-	0.013	0.75	46.81	0.3	1.08	0.76	4431	13.85	898
<b>7<sup>th</sup> July</b>	128	23	0.35	0.29	0.48	0.17	0.011	0.83	47.42	0.17	0.76 - 0.99	0.91 - 0.99	2836 - 6263	12.35	712
<b>8<sup>th</sup> July</b>	215	30	0.38	0.29	0.55	0.17	0.003	0.41	14.63	0.08	0.2 - 0.69	0.24 - 0.69	1004 - 3131	14.67	768
<b>9<sup>th</sup> July</b>	198	38	0.46	0.09	0.53	0.25	-	-	-	-	-	-	-	-	-



773

774 **Figure 1**

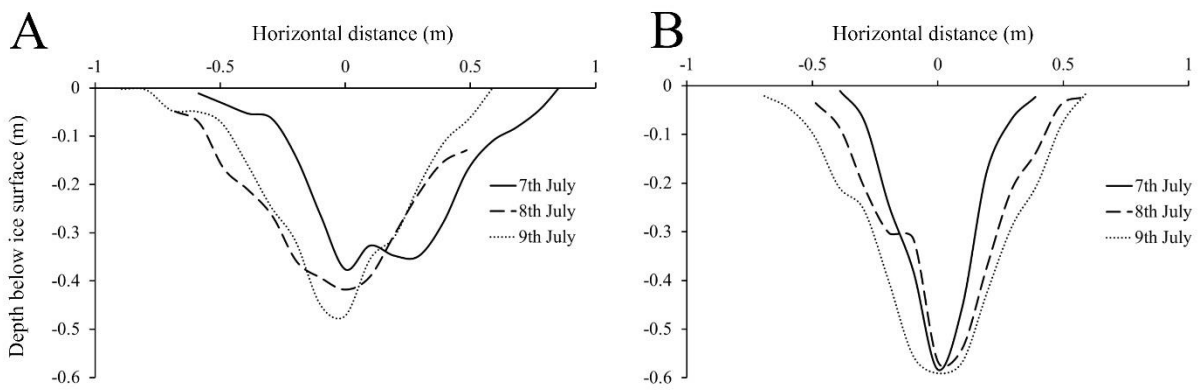
775



776

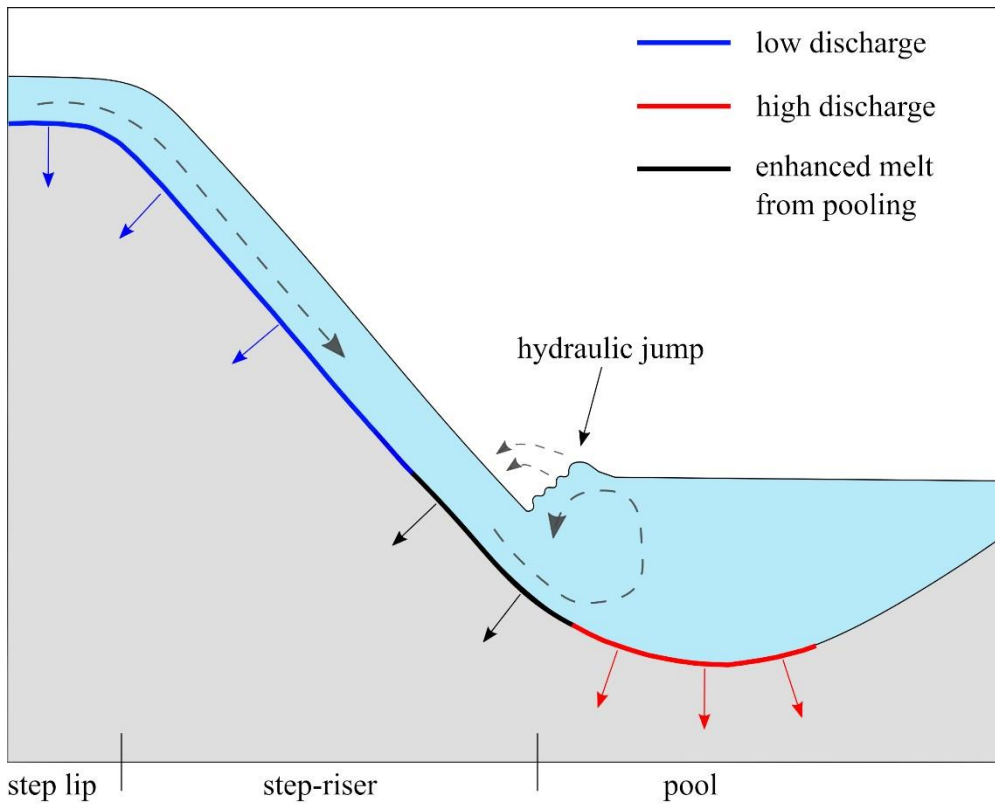
777 **Figure 2**

778



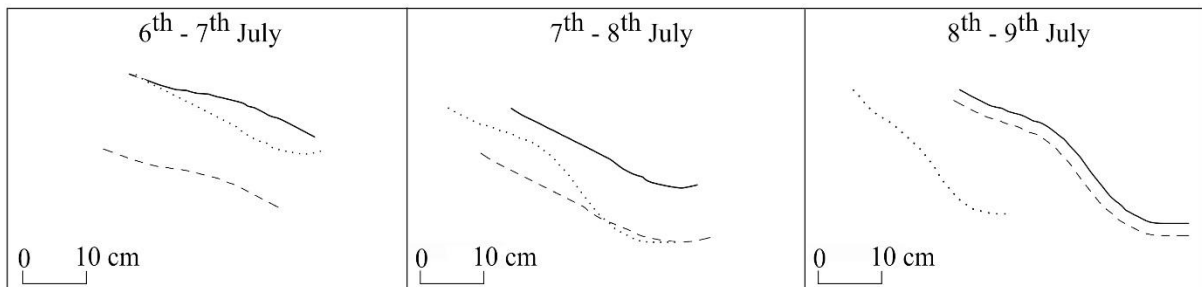
779

780 **Figure 3**



781

782 **Figure 4**



- original
- ..... end
- - - model

783

784 **Figure 5.**

785

786

787

788

789

790 **Figure 1.** (A) The red cross marks the field experiment location on Vadrec del Forno, with the  
791 location of the glacier within Switzerland inset. RapidEye imagery obtained from PlanetTeam  
792 (2017). (B) The stream reach planform, demonstrating the fracture and undulation troughs  
793 upstream of the knickpoint. Longitudinal foliation within the stream vicinity is oriented  
794 between  $58^\circ$  and  $89^\circ$  relative to north. Water and glacier flow is also to the north. Aerial  
795 imagery obtained from an elevation of 30 m at a resolution of 0.02 m using a DJI Phantom 3  
796 Series Standard quadcopter. (C) The step with the direction of water flow denoted by the black  
797 arrow. The 2.3 m long crevasse probe lying horizontal on the far stream bank provides scale.  
798 (D) Schematic longitudinal profile of the knickpoint, demonstrating the locations at which  
799 cross-section geometry and step height was measured, with an example cross-section inset.

800 **Figure 2.** Central step-riser profiles for each day demonstrating the recession and morphology  
801 of the step face immediately downstream of the step lip. The graph origin denotes the location  
802 of the original step lip (6<sup>th</sup> July). To facilitate direct comparison, profiles have not been  
803 corrected for vertical lowering.

804 **Figure 3.** Channel cross-sections measured on different days illustrating changes above (A)  
805 and below (B) the knickpoint. The direction of flow is into the page. Cross-sections are  
806 geometrically accurate relative to the glacier surface at the time of measurement, with the  
807 x-axis denoting lateral distance from the thalweg.

808 **Figure 4.** Schematic illustration of the differing zones of erosion across the knickpoint at  
809 varying discharges. The solid arrows denote the direction of boundary erosion and the dashed  
810 arrows denote the direction of water flow.

811 **Figure 5.** Observed and modelled knickpoint evolution for each day, showing the original  
812 knickpoint profile (as recorded on the start date), the end profile (as recorded on the end date)  
813 and the modelled profile derived from 18-hour melt rates.

814